Anal. Chem. **2000,** *72,* 791−799

Collision-Induced Dissociation of Ions within the Orifice−Skimmer Region of an Electrospray Mass Spectrometer

Bradley B. Schneider and David D. Y. Chen*

Department of Chemistry, University of British Columbia, Vancouver, BC, Canada V6T 1Z1

An equation was derived to describe the variation of the gas number density within the region between the orifice and the skimmer of an electrospray ionization mass spectrometer. The equation was used to develop a semi-quantitative model to predict the value of orifice voltages that lead to ion fragmentation within this region. This model made it possible to predict the types of solvent adducts observed for analytes at various orifice voltages. In addition, it is shown that a small number of high-energy collisions is equally effective for collision-induced dissociation as compared to a large number of low-energy collisions. Finally, this model is tested with different background electrolyte solutions and a different electrospray mass spectrometer. It is demonstrated that controlled fragmentation studies can be performed on single-quadrupole mass spectrometers, and the proposed model gives a reasonable description of the fragmentation process in both spectrometers.

Electrospray ionization mass spectrometry (ESI-MS) is a powerful technique that generates large intact molecules in the gas phase and is especially useful for the analysis of biomolecules. The benefits of ESI include the ability to multiply charge macromolecules and directly obtain mass information, the small sample requirement, and its compatibility with high-resolution separation techniques such as capillary electrophoresis (CE). Electrospray ionization has been widely applied in the analysis of proteins and peptides with many different types of mass analyzers, including quadrupoles,[1−6] time-of-flight,[7,8] and trapping devices.[9,10] CE/ESI-MS has been used for the analysis of oligonucleotides,[11,12] amino acids,[13] illicit drugs,[14,15] chiral drug mixtures,[16] steroids,[17] and low molecular mass compounds.[18] It is generally accepted that the ions observed in the gas phase by mass spectrometry are related to the species in the analyzed solution. However, the observed gas-phase charge states can be different from what is present in the aqueous phase.[19,20]

Ions are generated in electrospray ionization by one of two mechanisms, ion evaporation or Coulombic fissions of highly charged solvent droplets. These ions can remain solvated as they enter the ion sampling or interface region of the mass spectrometer. In the region prior to the skimmer, final desolvation occurs due to the heating of an ion by collisions with the background curtain gas. A curtain gas is typically an inert gas such as nitrogen that flows in front of the orifice of a mass spectrometer to prevent solvents and impurities from entering the high-vacuum region of the instrument. It is also possible to fragment ions by application of a strong electric field between the orifice and the skimmer. This region is therefore very important in generating the analyte ions that are presented to the mass analyzer. Due to the complexity of the processes occurring between the orifice and the skimmer, a quantitative model is not currently available to describe the input of energy that an ion receives due to collisions. Therefore, it is difficult to predict what fragmentation may occur, if any, before the analyte ions are presented to the mass analyzer.

With the advent of the triple-quadrupole mass spectrometer for tandem mass analyses, the role of the orifice−skimmer region in electrospray ionization has mainly been for the desolvation of desired ions. This is because a triple-quadrupole mass spectrometer allows for very precise control over the conditions for collision-

* To whom correspondence should be addressed: (e-mail) chen@chem.ubc.ca; (tel) (604) 822-0878; (fax) (604) 822-2847.

(1) Smith, R. D.; Loo, J. A.; Barinaga, C. J.; Edmonds, C. G.; Udseth, H. R. *J. Chromatogr., A* **1989**, *480*, 211−232.
(2) Konermann, L.; Collings, B. A.; Douglas, D. J. *Biochemistry* **1997**, *36*, 5554−5559.
(3) Light-Wahl, K. J.; Schwartz, B. L.; Smith R. D. *J. Am. Chem. Soc.* **1994**, *116*, 5271−5278.
(4) Davis, M. T.; Stahl, C.; Hefta, S. A.; Lee, T. D. *Anal. Chem.* **1995**, *67*, 4549−4556.
(5) Smith, R. D.; Udseth, H. R.; Barinaga, C. J.; Edmonds, C. G. *J. Chromatogr.* **1991**, *559*, 197−208.
(6) Pleasance, S.; Thibault, P.; Kelly, J. *J. Chromatogr.* **1992**, *591*, 325−339.
(7) Lazar, I. M.; Lee, E. D.; Rockwood, A. L.; Lee, M. L. *J. Chromatogr., A* **1997**, *791*, 269−278.
(8) Palmer, M. E.; Clench, M. R.; Tetler, L. W.; Little, D. R. *Rapid Commun. Mass Spectrom.* **1999**, *13*, 256−263.
(9) Figeys, D.; Aebersold, R. *Electrophoresis,* **1997**, *18*, 360−368.
(10) Figeys, D.; Aebersold, R. *Anal. Chem.* **1997**, *69*, 3153−3160.
(11) Bayer, E.; Bauer, T.; Schmeer, K.; Bleicher, K.; Maier, M.; Gaus, H. J. *Anal. Chem.* **1994**, *66*, 3858−3863.
(12) Cheng, X.; Gale, D. C.; Udseth, H. R.; Smith, R. D. *Anal. Chem.* **1995**, *67*, 586−593.
(13) Mansoori, B. A.; Volmer, D. A.; Boyd, R. K. *Rapid Commun. Mass Spectrom.* **1997**, *11*, 1120−1130.
(14) Tang, L.; Kebarle, P. *Anal. Chem.* **1993**, *65*, 3654−3668.
(15) Gaus, H. J.; Gogus, Z. Z.; Schmeer, K.; Behnke, B.; Kovar, K. A.; Bayer, E. *J. Chromatogr., A* **1996**, *735*, 221−226.
(16) Sheppard, R. L.; Tong, X.; Cai, J.; Henion, J. D. *Anal. Chem.* **1995**, *67*, 2054−2058.
(17) Warriner, R. N.; Craze, A. S.; Games, D. E.; Lane, S. J. *Rapid Commun. Mass Spectrom.* **1998**, *12*, 1143−1149.
(18) Wheat, T. E.; Lilley, K. A.; Banks, J. F. *J. Chromatogr., A* **1997**, *781*, 99−105.
(19) Konermann, L.; Douglas, D. J. *Biochemistry* **1997**, *36*, 12296−12302.
(20) Carbeck, J. D.; Severs, J. C.; Gao, J.; Wu, Q.; Smith, R. D.; Whitesides, G. *J. Phys. Chem. B* **1998**, *102*, 10596−10601.

10.1021/ac990926t CCC: $19.00
Published on Web 01/19/2000

induced dissociation (CID) of an ion in the collision cell. A constant background gas pressure can be maintained throughout the collision cell, yielding a constant mean free path and an easily quantifiable number of collisions. Also, this pressure can be varied in a controlled manner to increase or decrease the number of collisions. The precise control of CID parameters, such as ion energy, background pressure, and mass of the target gas, in a triple-quadrupole instrument makes it much more desirable for tandem mass analyses than the more complicated processes occurring in the orifice−skimmer region of a single-quadrupole electrospray mass spectrometer. Also, precursor ions are mass selected prior to entering the collision cell. However, controlled fragmentation in the orifice−skimmer region of a single-quadruple mass spectrometer is also very useful, particularly when only one analyte species is present, such as in CE/MS. In addition, it is imperative to understand the whole process of the production of ions in the mass spectrometer when dealing with complex biological samples, even when a triple-quadrupole mass spectrometer is available.

Although electrospray is a soft ionization source, ions can be fragmented in the orifice−skimmer region, and sometimes structural information about a particular ion can be obtained. The typical method for fragmenting ions involves increasing the electric field strength between the orifice and skimmer until fragmentation is observed. In many instances, the actual processes occurring to achieve fragmentation are poorly understood.

This paper describes the first attempt to semiquantitatively predict the electric field strengths necessary for collision-induced dissociation of ions within the orifice−skimmer region. The process of a gas expanding from atmospheric pressure into vacuum is reviewed, and a mathematical model is derived to determine the variation of background gas pressure within a free jet expansion for the two mass spectrometers used in this study. The model yields an estimate of the orifice voltages necessary for the onset of ion fragmentation.

Related publications have focused on determining the number of collisions occurring inside a free jet expansion within the interface region of an inductively coupled plasma mass spectrometer[21] and visualizing shock waves formed at the surface of the skimmer.[22] Neither of these studies involves electrospray ionization, but they both provide some insight into the free jet expansion within the orifice−skimmer region of a mass spectrometer.

EXPERIMENTAL SECTION

Chemicals and Apparatus. α- and β-cyclodextrin of 98% purity were purchased from Sigma (St. Louis, MO). γ-Cyclodextrin of 99% purity was a gift from Beckman Instruments (Fullerton, CA). Cyclodextrins were dissolved in 0.01 M certified ACS grade ammonium acetate obtained from BDH Chemicals (Toronto, ON, Canada). HPLC grade methanol and glacial acetic acid were obtained from Fisher Scientific Ltd. (Nepean, ON, Canada).

The instruments used for this study were a prototype single-quadrupole ion spray mass spectrometer and a prototype triple-quadrupole ion spray mass spectrometer both from Sciex (Thornhill, ON, Canada). A reduced liquid flow electrospray source was used for these studies with a home-built pressure system. The electrospray capillary was made with a 50 cm long fused-silica capillary having a 50 μm internal diameter and 150 μm external diameter (Polymicro Technologies, Phoenix, AZ). This capillary was connected with a 4 cm tapered tip, inside a 2 cm piece of stainless steel syringe tube with an inner diameter of 0.007 in. and an outer diameter of 0.014 in., (Small Parts Inc, Miami Lakes, FL). The junction was held together and sealed with epoxy glue. The tapered spray tips were pulled in-house and had an internal diameter at the tip of ∼20 μm. A voltage of 3 kV was applied for electrospray with a constant curtain gas flow of ∼1 L/min as measured by a series FM-1050 gas flow meter (Matheson, Montgomeryville, PA). Medical grade nitrogen from Praxair (Mississauga, ON, Canada) was used as the curtain gas for the single-quadrupole system and ultrahigh-purity nitrogen from Praxair for the triple-quadrupole system. A syringe pump (Harvard Apparatus syringe infusion pump 22, South Natick, MA) was used to generate a solution flow rate of 0.2 μL/min.

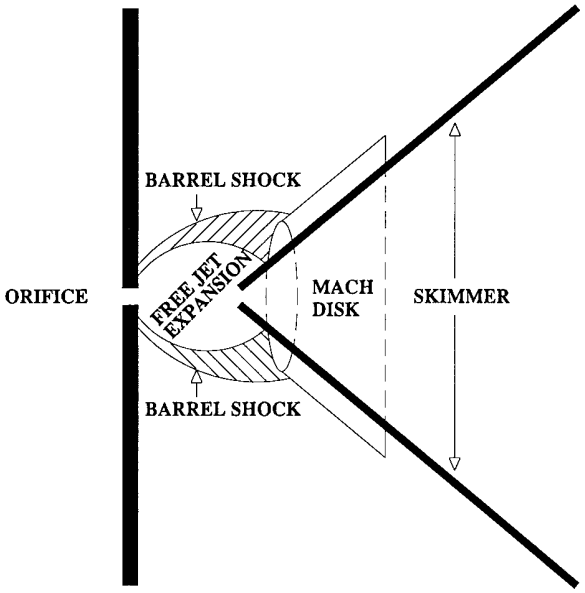

Figure 1. Scaled structure of a free jet expansion within the orifice−skimmer region of an electrospray mass spectrometer.

RESULTS AND DISCUSSION

The gas flow from atmosphere through the ion sampling orifice into the first vacuum stage of an electrospray mass spectrometer forms a free jet (Figure 1). The enthalpy of the gas in the source region of a free jet is converted into directed bulk flow kinetic energy. This results in a decrease in the local gas temperature throughout the free jet as shown in eq 1, where T is the

$$T = T_0(1 + 0.5(\gamma - 1)M_{\text{eff}}^{\ 2})^{-1} \qquad (1)$$

temperature at a given point in the free jet, T_0 is the source temperature, γ is the ratio of heat capacity at constant pressure to heat capacity at constant volume (C_p/C_v), and M_{eff} is the local mach number, or the calculated ratio of the gas flow speed to the local speed of sound. For the two mass spectrometers used in this study, the temperature in the expansion decreases from 295 K at the sampling orifice to ∼10 K near the skimmer. When the

(21) Douglas, D. J.; French, J. B. *J. Anal. At. Spectrom.* **1988**, *3*, 743−747.
(22) McMichael, G. E.; French, J. B. *Phys. Fluids* **1966**, *9*, 1419−1420.

temperature of the gas decreases, the local speed of sound of the gas also decreases, as shown in the following equation:

$$a = \sqrt{\gamma kT/m} \tag{2}$$

where a is the speed of sound of the gas, k is Boltzmann's constant, T is the temperature, and m is the mass of the atom or molecule. Because of the gas acceleration, at some point downstream in the free jet, the speed of the gas molecules will exceed the local speed of sound. The Mach number in the expansion is given by

$$M = A\left(\frac{x - x_0}{D}\right)^{\gamma-1} - \frac{1}{2}\left(\frac{\gamma+1}{\gamma-1}\right)/A\left(\frac{x - x_0}{D}\right)^{\gamma-1} \tag{3}$$

where A and x_0 are constants that are dependent on the value of γ,[23] D is the orifice diameter, and x is the distance downstream from the start of the free jet. Nitrogen ($\gamma = 1.4$) was used as the curtain gas in this study. A Mach number of 1, where the gas speed is equal to the local speed of sound of the background gas, is achieved within approximately 3/4 of an orifice diameter. At this point, the local pressure within the free jet has dropped to 64% of its initial atmospheric pressure. At points farther downstream in the free jet, the gas speed is supersonic. The maximum Mach numbers achieved on the single- and triple-quadrupole mass spectrometers were 7.3 and 9.4, respectively.

The gas number density within a free jet is proportional to the inverse square of the linear distance from its origin. The free jet is surrounded by a barrel shock and terminated by a shock wave known as the Mach disk.[24] Inside the Mach disk, the directed bulk flow of the molecules and atoms in the free jet is rerandomized, and the temperature increases to approximately the temperature of the source. The distance from the orifice to the Mach disk (x_m) is given by[23]

$$x_m = 0.67 D_0 \sqrt{(p_0/p_1)} \tag{4}$$

where p_0 is the pressure in the source region, p_1 is the pressure within the expansion region, and D_0 is the diameter of the orifice.

Inside the Mach disk of a free jet expansion, it becomes difficult to model the behavior of ions and neutral molecules. For this reason, it is necessary to calculate the location of the Mach disk by eq 4 to ensure that the skimmer is located within the free jet. The source pressure was ~760 Torr, and the pressure between the skimmer and the orifice was approximately 5 and 2 Torr for the single- and the triple-quadrupole systems, respectively. The orifice diameters were measured to be ~0.25 mm on the two mass spectrometers used in this study. The distances from the orifice to the Mach disk were calculated to be 2.11 and 3.27 mm, respectively for the single- and triple-quadrupole instruments. Since the measured distance from the orifice to the skimmer was only 1.7 mm for the single-quadrupole and 3 mm for the triple-quadrupole instrument, the area where the collisions of analyte ions and gas molecules occur is still inside the free jet region. If a free jet is prematurely terminated at a blunt surface, the motion of the gas molecules will rerandomize, resulting in the early formation of a shock wave. A cone-shaped skimmer is intended to prevent this from occurring.

The theory of gas dynamics can be applied to the sampling region of an electrospray ionization mass spectrometer. The source region is the area before the orifice plate, where the pressure is 760 Torr, and the expansion region is the area between the orifice and the skimmer. The gas number density along a streamline in a free jet is given by[24]

$$\frac{n_0}{n_i} = \left(1 + \frac{\gamma - 1}{2} M^2\right)^{1/\gamma - 1} \tag{5}$$

where n_0 is the number density of the gas within the source region, n_i is the number density at some point within the free jet, and M is the Mach number. Equation 3 was solved by inserting the parameter values relevant to the two mass spectrometers. For nitrogen ($\gamma = 1.4$), the values of A and x_0 are 3.65 and 0.40D, respectively, where D is the orifice diameter.[23] The solution of eq 3 with these values yields eq 6.

$$M = 3.65\left(\frac{x - 0.01}{0.025}\right)^{0.4} - 0.8220\left(\frac{x - 0.01}{0.025}\right)^{-0.4} \tag{6}$$

This simplified equation was substituted into eq 5 to solve for n_i.

$$n_i = n_0 / \left(2.6645(39.2157x - 0.4)^{0.8} + \frac{0.1351}{(39.2157x - 0.4)^{0.8}} - 0.2\right)^{2.5} \tag{7}$$

Solving this equation over small increments allows us to determine the number density along any streamline of the free jet. Because both eqs 3 and 5 depend on γ, different curtain gases will lead to different equations for number density in a free jet.

Due to the complexity of eq 7, we decided to solve for the total number of collisions within the free jet by dividing the region between the orifice and the skimmer into 10 μm increments. To obtain the average number densities, the initial x value used was 0.0142 cm, corresponding to the beginning of the region where the pressure decreased with an inverse square relationship to the distance from the orifice. The number density for region two was then calculated by substituting an x value of 0.0152 cm into eq 7. The average number density within each of these regions is shown in Figure 2. The free jet forms at a certain position behind the orifice, and during the expansion, the gas density is inversely proportional to the square of the distance from the orifice. There are 2.5×10^{19} molecules/cm^3 under atmospheric pressure, and the number density drops to 5.83×10^{16} molecules/cm^3 in front of the skimmer cone of the single-quadrupole instrument. For the triple-quadrupole mass spectrometer, the density at the skimmer drops to 1.73×10^{16} molecules/cm^3. The background pressure

(23) Ashkenas, H.; Sherman, F. S. The Structure and Utilization of Supersonic Free Jets in Low-Density Wind Tunnels. In *Fourth International Symposium on Rarefied Gas Dynamics*; Deleeuw, J. H., Ed.; Academic Press: New York, 1965; Vol. 2, pp 84−105.

(24) Douglas, D. J. Fundamentals of Inductively Coupled Plasma−Mass Spectrometry. In *Inductively Coupled Plasmas in Analytical Atomic Spectrometry*, 2nd ed.; Montaser, A., Golightly, D. W., Eds.; VCH Publishers: New York, 1992; pp 613−650.

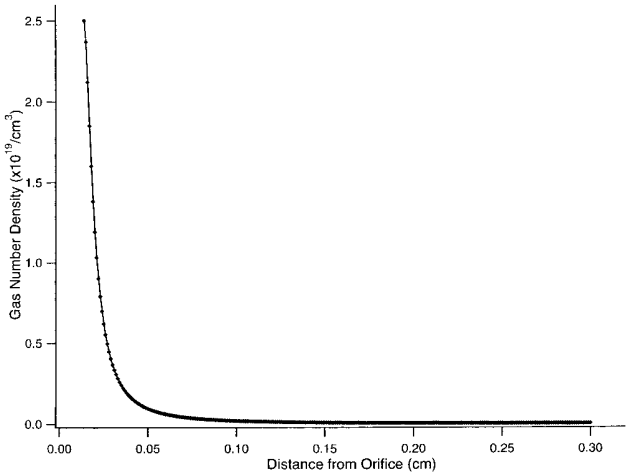

Figure 2. Variation of gas number density at various distances from the start of the free jet within the orifice−skimmer region of the triple-quadrupole mass spectrometer.

between the orifice and the skimmer outside of the barrel shock is substantially higher than the pressure within the free jet expansion. The number density obtained by eq 7 is extremely important because it allows us to determine the number of collisions in the free jet region and, therefore, allows us to estimate the amount of translational energy being converted into internal energy for unimolecular dissociation.

The mean free path is the average distance an analyte can travel before colliding with a gas molecule and is given by

$$\lambda = \frac{1}{n\sigma}(1 + v/c) \tag{8}$$

where λ is the mean free path in the laboratory frame of reference, n is the number density, σ is the collisional cross section for the ion and the target gas molecule, v is the velocity of the expansion gas flow, and c is the velocity of the ion in the gas frame of reference. The gas flow velocity was determined from eq 9

$$v_{\text{flow}} = Ma \tag{9}$$

where M is the mach number and a is the local speed of sound determined from eq 2. The ion velocity was determined using eq 10:

$$c = (2E/m)^{1/2} \tag{10}$$

where c is the ion velocity in the gas frame of reference, m is the mass of the ion, and E is the translational energy of the ion. In this case, the collisional cross section was calculated by

$$\sigma = \pi(r_1 + r_2)^2 \tag{11}$$

where r_1 and r_2 are the cross-sectional radii of the two molecules involved in the collision. The diameter of a nitrogen gas molecule was estimated to be 1.49 Å from its covalent radius, and the diameters of α-, β-, and γ-CD have previously been determined to be 1.37, 1.53, and 1.69 nm, respectively.[25] The collisional cross sections used for this model were 218.9, 262.9, and 310.9 Å, respectively. At high orifice voltage on the single-quadrupole mass spectrometer, the cross section for β-CD generated an average of 371 collisions/10 μm region at the start of the free jet, and an average of 1 collision in the 10 μm region prior to the skimmer. The number of collisions was slightly greater for γ-CD and slightly smaller for α-CD. The collisional cross sections were assumed to remain constant throughout the orifice−skimmer region. In reality, the collisional cross sections decrease in magnitude throughout this region until complete ion desolvation is achieved. This decreasing ion diameter was not accounted for in this model and is a potential source of error.

Each of the 10 μm regions was then further divided to attain even smaller regions with the length of one mean free path, thus containing only one collision between the ion and a gas molecule. This was accomplished by adding the calculated mean free path at the start of a region with the distance from the orifice to yield the start of a new region. The number densities were calculated by eq 7 for each of the new smaller regions obtained in this way. By repeating this procedure for all of the regions between the orifice and the skimmer, a large spreadsheet is obtained with each row corresponding to one collision.

Collision Dynamics. Collisions occur between the analyte and the neutral curtain gas molecules, and these collisions convert kinetic energy into internal energy of the complex. The simplest way to model these collisions is to use a coordinate system that moves with the center of mass of the target and the molecule. This center of mass coordinate system has been described previously.[26] The kinetic energy of an ion after a collision, or its translational energy in the gas frame of reference, is described by

$$E_{\text{gas}} = E^0_{\text{gas}} + q\Delta V - E_{\text{loss}} \tag{12}$$

where $E°$ is the initial energy of the ion, q is the charge on the ion, ΔV is the potential difference the ion is accelerated through, and E_{loss} is the translational energy which the ion loses in the collision. In the laboratory frame of reference, the kinetic energy of the ion is slightly higher by a factor of v_{flow}. Since the factor v_{flow} contributes equally to the speed of both the cyclodextrin ions and the target gas molecules, it is important to model these collisions in the gas frame of reference. The energy available for conversion to internal energy, is the center of mass (CM) energy, E_{cm}, given by[26]

$$E_{\text{cm}} = (m_2/(m_1 + m_2))E_{\text{gas}} \tag{13}$$

where m_2 is the mass of the target gas molecule and m_1 is the mass of the ion. The summation of eq 13 over all of the collisions gives the total energy available for conversion to internal energy of the analyte ion. Two assumptions are made at this point. The first is that the collisions are highly inelastic, and the second is that all collisions are head-on, rather than glancing collisions,

(25) Bresolle, F.; Audran, M.; Pham, T. N.; Vallon, J. J. *J. Chromatogr., B* **1996**, *687*, 303−336.
(26) Douglas, D. J. *J. Am. Soc. Mass Spectrom.* **1998**, *9*, 101−113.

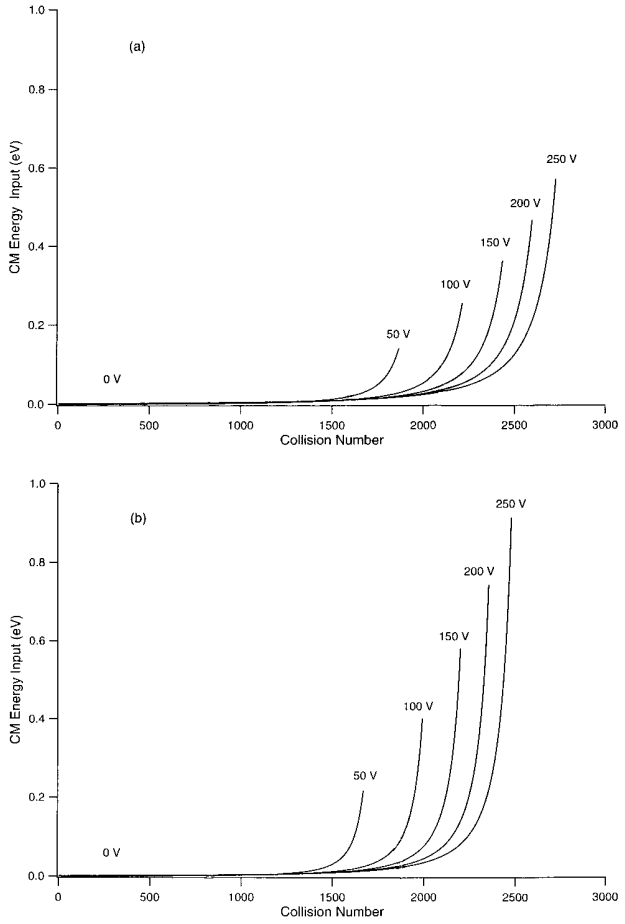

Figure 3. Center of mass energy per collision for β-CD at varying orifice voltages on the single-quadrupole mass spectrometer (a) and the triple-quadrupole mass spectrometer (b).

allowing the maximum energy to be converted. When an analyte ion strikes a nitrogen gas molecule, some of the translational energy of the complex is converted to internal energy. As many more of these low-energy collisions occur, the internal energy of the analyte ion builds up, causing it to dissociate before reaching the mass analyzer. Equation 13 was used to determine how much of the laboratory energy of an ion was converted into its center of mass energy. Each collision was treated as an inelastic collision between a moving ion and a stationary target gas molecule, and all of the center of mass energy was assumed to be converted into the internal energy of the analyte ion. This is reasonable for macromolecules such as the cyclodextrins used in this experiment.[27] It is apparent from eq 13 that heavier curtain gas molecules and higher ion energies favor more extensive fragmentation. The center of mass energy was determined for the ion in each of the increments. Plots of the center of mass energy attained by a β-CD ion per collision in the single- and the triple-quadrupole mass spectrometer are given in panels a and b of Figure 3, respectively. This figure shows that only the collisions occurring just before the skimmer are capable of imparting high levels of energy into the internal energy of an ion. The reason is the large mean free path an ion experiences in this region allows it to accelerate for a much longer distance under the influence of the electric field between the orifice and the skimmer. This leads to an increase in the laboratory energy of an ion and, thus, to an increased conversion of energy to center of mass energy for each collision with the background gas. Figure 3 also shows that as a larger voltage difference is utilized between the orifice and the skimmer on the two mass spectrometers, more collisions occur between an ion and the curtain gas. This is a result of the decreased mean free path in the laboratory frame of reference, because of the increased ion velocity in the gas frame. This also leads to the surprising result that an ion experiences more collisions within the orifice−skimmer region of the single-quadrupole mass spectrometer than the triple-quadrupole mass spectrometer. Due to the identical orifice diameters, and atmospheric pressure, the gas flow velocity (v_{flow}) within the free jet is identical on both mass spectrometers. With an orifice−skimmer voltage difference of 250 V, the electric field in this region is 1470.6 V/cm on the single-quadrupole system, and 833.3 V/cm on the triple-quadrupole system, and as a result, the ion velocity is much greater on the former.

Figure 4 illustrates the CM energy input to an ion in every 80 μm region from the start of the free jet in the single-quadrupole mass spectrometer. This figure illustrates that, in each of the regions, a similar amount of internal energy is generated through the collisions. In the first 80 μm region, hundreds of low-energy collisions occur to impart approximately the same amount of internal energy to an ion as the 9 or 10 high-energy collisions that occur in the 80 μm region prior to the skimmer. The graphs fluctuate near the final regions due to the varying numbers of collisions within the 80 μm increments determined by the average mean free path. Some regions have a variation of one or two extra collisions, which makes a greater difference near the skimmer, where there are few total collisions. The data for zero voltage difference between the orifice and the skimmer show that the β-CD molecule only has thermal energy. The thermal translational energy is calculated to be 0.0375 eV by the equipartition theorem, which is based upon three degrees of freedom for the translational energy of a gas molecule.[28] As an ion with thermal translational energy travels through the region in the free jet, very little energy is converted from translational to internal energy, preventing the occurrence of desolvation. Also, the ion signal is very weak due to the lack of electric field which is required to propel an ion past the skimmer into the Q0 region of the mass spectrometer. The ion undergoes a few initial collisions and then is swept along with the expansion gas (v_{flow}). On the other hand, with an increase in electric field, the laboratory energy of the complex also increases and so does the center of mass energy. Therefore, at a 250 V difference between the orifice and skimmer, a large amount of CM energy is generated in all of the regions.

The ratio of the kinetic energies of an ion after and before a collision with a stationary gas molecule is given by[29]

$$\frac{E'_{gas}}{E_{gas}} = \frac{m_1^2 + m_2^2}{m^2} - \frac{m_2 E_{cm}}{m E_{gas}} + \frac{2m_1 m_2}{m^2}\sqrt{\left(1 - \frac{E_{cm} m}{E_{gas} m_2}\right)}(\cos\theta_{cm}) \quad (14)$$

(27) Marzluff, E. M.; Campbell, S.; Rodgers, M. T.; Beauchamp, J. L. *J. Am. Chem. Soc.* **1994**, *116*, 6947−6948.

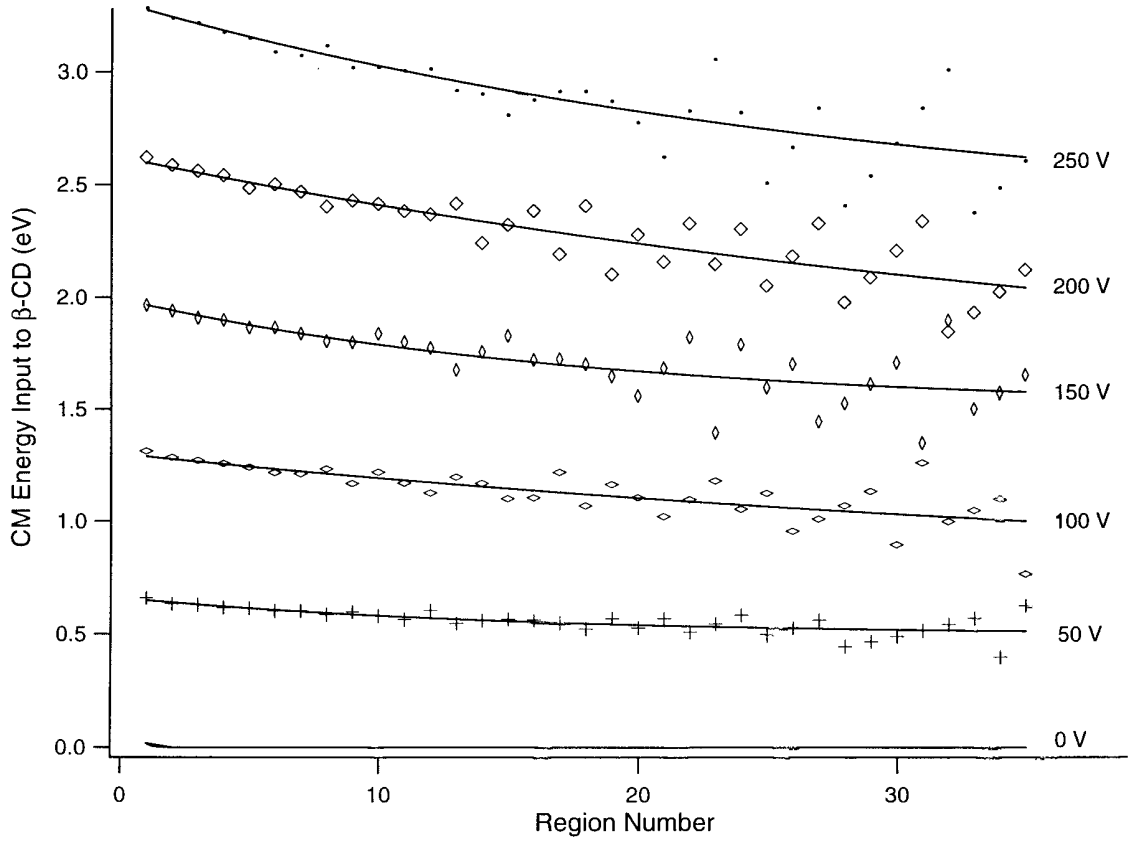

Figure 4. Center of mass energy converted to internal energy of a β-CD ion per 80 μm region from the origin of the free jet on the single-quadrupole mass spectrometer. The data pertaining to orifice−skimmer voltage differences of 250, 200, 150, 100, 50, and 0 V are illustrated.

where E'_{gas} and E_{gas} represent the translational energy of the ion in the gas coordinate system after and before a collision, respectively. The sum of the masses of the ion and the gas molecule is m, and θ_{cm} is the scattering angle of the ion in the center of mass coordinate system. After a collision with a stationary gas molecule, an energetic ion loses some of its translational energy to both the ion internal energy and to the recoil of the stationary target gas molecule.[29] Equation 14 applies to both elastic and inelastic collisions. For the model used here, eq 13 and eq 14 were combined to describe an inelastic collision.

$$E'_{gas}/E_{gas} = m_1^2/m^2 \qquad (15)$$

This equation was used to determine the ion translational energies (E'_{gas}) after each of the collisions. These energy values were then used as the new initial translational energy for the next collision.

A plot of the calculated internal energy of a β-CD ion versus the orifice voltage of the single-quadrupole system is shown in Figure 5. The skimmer was maintained at a potential of 0 V for the single-quadrupole, and 110 V for the triple-quadrupole system. As expected, an increase in the magnitude of the electric field in the orifice−skimmer region led to a linear increase in the amount of internal energy gained by the ion on both instruments. Due to the smaller droplets generated by the reduced-flow electrospray source, desolvation was achieved with an approximate internal

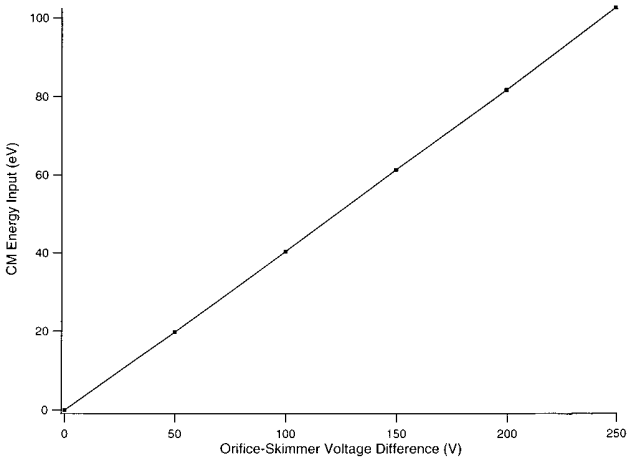

Figure 5. Energy converted to internal energy of the β-cyclodextrin complex versus the orifice potential applied on the single-quadrupole mass spectrometer.

energy of 20 eV for the single-quadrupole and 12 eV for the triple-quadrupole instrument. This value is expected to be substantially less than that required for conventional ion spray systems, and the discrepancy between machines indicates a different efficiency in desolvation from the curtain gas for the triple-quadrupole system or an electrospray source generating ions with varying degrees of solvation. Another possibility is a less accurate curtain gas flow meter on the single-quadrupole instrument or a slight difference in sprayer position between instruments. Since the

(28) Atkins, P. W. *Physical Chemistry*; Oxford University Press: New York, 1994.
(29) Covey, T.; Douglas, D. J. *J. Am. Soc. Mass Spectrom.* **1993**, *4*, 616−623.

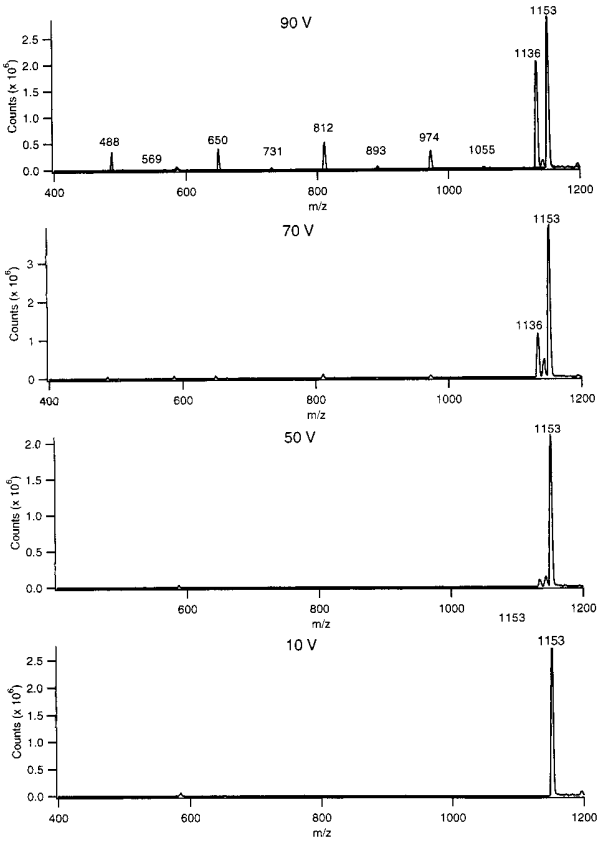

Figure 6. Mass spectra obtained for β-CD in ammonium acetate solutions at various orifice−skimmer voltage differences, 10, 50, 70, and 90 V, on the triple-quadrupole MS. Peak identification: β-CD·ammonium (1153), β-CD·proton (1136), and protonated fragments (488, 650, 812, 974 *m*/*z*). The mass spectra at high orifice voltages show the presence of low-intensity, doubly charged dimer fragments at 569, 731, 893, and 1055 *m*/*z*. The peak at 1144 *m*/*z* pertains to a doubly charged dimer of β-CD.

initially generated droplets are much smaller than usual with the reduced-flow source, less heating of a molecule is necessary for desolvation. A maximum orifice voltage of 250 V was used for this study, and extensive fragmentation was possible with these electric field strengths. This maximum was chosen due to the electrical breakdown of the gas between the orifice and the skimmer at higher voltages. This was evident by very extensive fragmentation, strong ion signals, and a small pinpoint of bright light observed near the orifice plate on the single-quadrupole mass spectrometer.

The behavior of ions from cyclodextrins in ammonium acetate was monitored by the mass analyzer when the orifice voltage was varied. At low orifice voltages, a single peak is obtained at 991, 1153, and 1315 *m*/*z* for the α-, β-, and γ-cyclodextrins, respectively. These correspond to the singly charged cyclodextrin complexes with an ammonium adduct. As the orifice voltage increases, protonated cyclodextrin complexes are observed. Finally, at higher orifice voltages, fragments of the sugar with decreasing numbers of glucose units are present as shown in Figure 6. All of these fragments are observed as protonated singly charged ions. At very high orifice voltages, low-intensity, doubly charged dimers are observed. For the cyclodextrin in acetic acid solutions, singly charged protonated molecular ions are observed at low voltages.

Table 1. Predicted and Observed Orifice−Skimmer Voltage Differences for the Two Mass Spectrometers (V)

process	single-quadrupole MS		triple-quadrupole MS	
	pred	exptl	pred	exptl
a. Values for α-CD				
desolvation	50	50	30	30
desolvation + H^+ transfer from NH_4^+	53.6	55	34.2	40
desolvation + H^+ transfer from NH_4^+ + dissociation	81.3	90	62.5	70
desolvation + dissociation in acetic acid	77.2	80	58.4	55
b. Values for β-CD				
desolvation	50	50	30	30
desolvation + H^+ transfer from NH_4^+	54.3	60	34.9	45
desolvation + H^+ transfer from NH_4^+ + dissociation	87.0	90	68.3	70
desolvation + dissociation in acetic acid	82.2	80	63.4	60
c. Values for γ-CD				
desolvation	50	50	30	30
desolvation + H^+ transfer from NH_4^+	55.0	75	35.6	55
desolvation + H^+ transfer from NH_4^+ + dissociation	92.7	90	74.0	75
desolvation + dissociation in acetic acid	87.1	85	68.4	65

Upon increasing the orifice voltage, fragmentation is induced, yielding singly charged protonated fragments. Experimental orifice voltages for proton transfer and decomposition in both ammonium acetate and acetic acid solutions are shown in Table 1 for the results obtained on both of the mass spectrometers. These values are tabulated for 10% conversion to fragments.

The desolvation energy was obtained by observation. Approximately 50 V was necessary on the orifice of the single-quadrupole instrument to achieve desolvation and maximum ion signals. For the triple-quadrupole system, a much smaller potential difference between the orifice and the skimmer was necessary (30 V). The formation of a proton adduct to β-CD was modeled as a proton transfer from an ammonium ion because the concentration of ammonium ions vastly exceeded the number of free protons. This transfer was believed to be an intramolecular transfer because it is unlikely that two cyclodextrin ions would collide within the free jet. The gas-phase proton affinity for ammonium is 205 kcal/mol or 8.89 eV/molecule.[30] The gas-phase proton affinity for the cyclodextrin complexes was approximated to be 200 kcal/mol or 8.67 eV/molecule. Proton adducts are most likely associated with the oxygen atoms of the glycosidic bonds along the rim of the basket-shaped CDs as a result of the C1 conformation of the glucose subunits.[31] The nonbonding electron pairs on these glycosidic oxygen bridges are directed toward the inside rim of the cyclodextrin cavity. These nonbonding electrons generate a high degree of electron density in this region and, consequently, some Lewis base character. The calculated energy required for this proton transfer was 0.217 eV/molecule. The bond

(30) Bowers, M. T. *Gas-Phase Ion Chemistry*; Academic Press Inc.: New York, 1979; Vol. 2.

(31) Szejtli, J. *Cyclodextrins and their Inclusion Complexes*; Akademiai Kiado: Budapest, 1982.

Table 2. Working Curves for Internal Energy vs Orifice Voltage for the Cyclodextrins in the Single-Quadrupole and the Triple-Quadrupole Mass Spectrometers

	E_{int}		
instrument	α-CD	β-CD	γ-CD
single-quadrupole MS	$0.4190V_{or} - 0.2854$	$0.4196V_{or} - 0.3423$	$0.4197V_{or} - 0.3741$
triple-quadrupole MS	$0.4095V_{or} - 0.3832$	$0.4107V_{or} - 0.4303$	$0.4118V_{or} - 0.5583$

strengths of the α-1,4 glycosidic linkages in β-CD were approximated from hydrolysis activation energies.[31] Fragments with successively fewer glucose subunits were observed, and this fragmentation pattern is in agreement with experimental observations from both radiolysis and hydrolysis. The glycosyl bond strength used in this study was characteristic of a nonenzymatic solution-phase hydrolysis value of ~34 kcal/mol, or 1.47 eV/molecule.[31]

The RRK rate equation was used to determine the kinetic shifts for the processes of proton transfer and bond dissociation. The heating of a complex via collisions occurs over its entire surface, and the energy is regarded as freely flowing between all of the harmonic oscillators in the complex. The rate constant (K) and the amount of energy that is necessary to cause bond dissociation has the following relationship in the RRK theory:[32]

$$K \approx \nu((E - E_0)/E)^{s-1} \qquad (16)$$

where K is the RRK rate constant for dissociation of the activated complex, ν is a vibrational frequency, E is the ion internal energy, E_0 is the bond strength, and s is the number of vibrational degrees of freedom. It has been found that the results obtained from eq 16 are closer to experimental results when half of the calculated number of vibrational degrees of freedom is used.[32] This correction was made for the calculations in this paper. The vibrational frequency used for this analysis was that of a fast vibration (10^{14} Hz). The use of large vibrational frequencies such as this is supported by work done using the blackbody infrared radiative dissociation (BIRD) technique.[33] The RRK rate constant used in this study was 10^3 s^{-1}. This value is necessary as it takes ~1 ms for an ion to travel from the interface region of the mass spectrometer to the detector, depending upon the ion energy. The total number of vibrational degrees of freedom was 375, 447, and 519 for the α-, β-, and γ-cyclodextrin, respectively.

The orifice voltages for the proton transfer and the dissociation of the cyclodextrin complexes can be predicted from the data in Table 2. These data are the working curves of internal energy input versus orifice voltage for the various cyclodextrins in the two mass spectrometers. By substituting the calculated energies for proton transfer and dissociation into the y variable (E_{int}) in these equations, it is possible to solve for the x variable, or the orifice voltage requirement for dissociation and proton transfer. These predicted orifice voltages were then compared to the experimental data, and the results are shown in Table 1. The predicted values showed good correlation with the experimentally determined values for the cyclodextrin complexes in both ammonium acetate and acetic acid. The predicted orifice voltage for dissociation of the cyclodextrins in acetic acid was ~10 V lower than that for the ammonium acetate due to the lack of proton-transfer energy required. The results obtained with the cyclodextrins in acetic acid remained consistent with the addition of up to 50% v/v methanol.

The effect of vibrational frequency on the predicted orifice voltages obtained using the RRK rate equation was tested by repeating the calculations with vibrational frequencies of 10^{13} and 10^{15} Hz. This uncertainty of 1 order of magnitude in the vibrational frequency was found to yield a difference of 3.1−11.2% for the predicted orifice voltages.

As previously mentioned, half of the total number of degrees of freedom was used in the RRK rate equation. To determine the amount of error incorporated into this model with the use of different values for vibrational degrees of freedom, the calculations were repeated using one-third the number of degrees of freedom. This deviation was found to yield decreases ranging from 5.7 to 13.8% for the predicted orifice voltages for β-CD.

Similarly, to determine the amount of error incorporated into these calculations by varying the value of the RRK rate constant, the calculations were repeated using K values of 10^2 and 10^4 s^{-1}. This deviation of 1 order of magnitude in the rate constant resulted in a 5% difference in the predicted orifice voltages.

A deviation from the calculated values was found for the proton-transfer energy of γ-CD. The predicted orifice voltage for proton transfer from ammonium to γ-CD was ~20 V less than that observed on both of the two mass spectrometers. The reason for this is believed to be the size of the cyclodextrin cavities. α-CD has a very small cavity, which increases its Lewis base capability due to increased localization of the nonbonding electron pairs on the glycosidic oxygen linkages. This causes the proton transfer from ammonium to be more favorable, and as a result, it occurs at a lower orifice voltage than predicted. γ-CD has a substantially larger cavity, which is not as receptive to proton transfer. The large cavity diameter positions the glycosidic linkages at a substantially greater distance from each other. This decreased localization reduces the Lewis base character of γ-CD relative to both α- and β-CD. As a result, more energy is necessary to drive proton transfer. This difference in proton-transfer energy was not accounted for in the model, and the proton affinity used here seems to have been most applicable for α-CD.

The accuracy of the predicted orifice voltages for dissociation increases with increasing size of the cyclodextrins. This is most likely a result of the assumption that 100% of the available center of mass energy is converted to internal energy of the ion. Marzluff et al. demonstrated that greater than 90% of the available center of mass energy is converted to internal energy with the nonapep-

(32) Laidler, K. J. *Theories of Chemical Reaction Rates*; Mcgraw-Hill Publishers: New York, 1969.

(33) Strittmatter, E. F.; Schnier, P. D.; Klassen, J. S.; Williams, E. R. *J. Am. Soc. Mass Spectrom.* **1999**, *10*, 1095−1104.

tide bradykinin.[27] This molecule has 444 internal degrees of freedom and is thus comparable to the β-CD used in this experiment. For smaller molecules, the conversion efficiency to internal energy has been found to be substantially less.[27] For this reason, the predicted orifice voltage requirement for dissociation of α-CD, with 375 internal degrees of freedom, is expected to be low. Similarly, the above approximation is expected to be most relevant for γ-CD because it is the largest of the sugars, with 519 internal degrees of freedom.

This model does not account for collisional cooling of the ions within the first rf-only quadrupole (Q0) located behind the skimmer. Collisional cooling is a process where ions lose translational energy via low-energy collisions within the Q0 rods. The purpose is to focus ions to the center of the axis between the rods, thus increasing ion transmission. Also, the decreased spread in the translational energy of the ions improves the resolution. Because an ion has been activated prior to arriving in Q0, the increase in internal energy due to these collisions is considered to be negligible. This is supported by the observation that, at low voltage differences between the orifice and the skimmer, ion fragmentation is not observed. For this reason, internal energy input to an ion must be minimal in comparison to that achieved between the orifice and the skimmer.

CONCLUSIONS

This free jet model allows for semiquantitative determination of the orifice voltage necessary to induce fragmentation of ions formed by ESI and may also be used for gas-phase binding studies. Premature fragmentation may not be desirable under many circumstances, so it is useful to be able to predict when fragmentation will start to occur and when only a parent ion will be observed by the mass analyzer. This model may prove to be extremely useful for the multitude of single-quadrupole instruments currently in operation and for choosing the optimum conditions in triple-quadrupole instruments. While these results are quite promising for large molecules, the model still needs to be tested in other systems to determine its general applicability.

ACKNOWLEDGMENT

The authors thank Dr. Don Douglas and Dr. Bruce Collings for their insightful discussions and technical assistance. The two mass spectrometers were kindly loaned to us from Dr. Don Douglas's research group. This work is supported by the Natural Sciences and Engineering Research Council of Canada.

Received for review August 17, 1999. Accepted November 30, 1999.

AC990926T